

**FABRICATION OF 3D POROUS BETA TRICALCIUM PHOSPHATE BONE
SCAFFOLD COATED BY POLY(VINYL ALCOHOL) AND
POLY(LACTIC ACID)**

by

WONG WAI YEE

**Thesis submitted in fulfillment of the requirements
for the degree of
Master of Science**

January 2017

ACKNOWLEDGEMENTS

First and foremost, I would like to express my gratitude to my helpful supervisor, Prof. Dr. Ahmad Fauzi Mohd. Noor for his continuous supervision, inspiration, patience and valuable time in guiding me throughout the entire duration to complete this research work. My sincere appreciation also to give to my co-supervisor Prof. Dr. Radzali Othman and Dr. Nurazreena bt. Ahmad for their constructive input in this project.

I would like to thank the School of Materials and Minerals Resources Engineering USM for providing me space and facilities to run this project and giving me a chance to complete my degree of Master of Science. Besides, my gratitude to all the administrative and technical staffs in School of Materials and Mineral Resources, USM for their assistance and technical support in operating machines during my research.

I would also like to acknowledge the financial support from Ministry of Higher Education Malaysia through MyMaster scheme (MyBrain15) as well as FRGS grant (203/PBAHAN/6071285).

I would like to take this opportunity to dedicate my appreciation to all my friends in USM, especially Ms. Farah, Ms. Azma Fatini, Ms. Harmiza, Ms. Chutathip and Mr. Zaw, who helped me, supported me and gave me strength in completing this project. Thank you very much.

Finally, I would like to send my greatest gratitude for my beloved family for their endless love, support and encouragement.

TABLE OF CONTENTS

	Page
ACKNOWLEDGEMENTS	ii
TABLE OF CONTENTS	iii
LIST OF TABLES	vii
LIST OF FIGURES	ix
LIST OF SYMBOLS	xiv
LIST OF ABBREVIATIONS	xv
ABSTRAK	xvi
ABSTRACT	xvii
CHAPTER ONE : INTRODUCTION	
1.1 Research Background	1
1.2 Problem Statement	3
1.3 Research Objective	5
1.4 Scope of Research	5
CHAPTER TWO : LITERATURE REVIEW	
2.1 Introduction	7
2.2 Hard Tissue Mineralisation	7
2.3 Natural Bone	9
2.4 Bone Remodeling	11
2.5 Bone Scaffold for Orthopaedic Treatment	13
2.6 Biomaterial	18
2.6.1 Bioceramics	20
2.6.1(a) Hydroxyapatite	22

2.6.1(b) Tricalcium Phosphate	22
2.6.2 Biopolymer	23
2.7 Calcium Phosphate Bioceramic/Biopolymer Scaffold	26
2.8 Fabrication of 3D Porous Scaffold	28
2.9 Scaffold Coating	29
2.10 β -TCP Sponge Coated Biopolymer	30
2.10.1 Polymeric Sponge Replica Method	31
2.10.2 Poly (Lactic Acid)	34
2.10.3 Poly (Vinyl Alcohol)	36
2.11 Summary	38
 CHAPTER THREE : MATERIALS AND METHODS	
3.1 Introduction	39
3.2 Materials	40
3.2.1 Fabrication of β -TCP scaffold	40
3.2.2 Biopolymer Coating	40
3.2.3 Simulated Body Fluid	40
3.3 Fabrication of β -TCP Scaffold via PU Sponge Replica Method	41
3.3.1 Effect of Sintering Temperature	44
3.3.2 Effect of β -TCP to Water Ratio	44
3.3.3 Effect of Binder Addition to β -TCP Slurry	45
3.3.4 Effect of Soaking Time of Sintering	46
3.4 Biopolymer Coating	47
3.4.1 β -TCP/PVA (Single Layer Coating)	48
3.4.1(a) Excess Polymer Solution Removal	49
3.4.2 β -TCP/PLA (Single Layer Coating)	51

3.4.3	β -TCP/PVA/PLA (Bi-layer Coating)	52
3.5	Characterisation Techniques	54
3.5.1	X-ray Diffraction	55
3.5.2	Fourier Transform Infra-Red Spectroscopy	55
3.5.3	Scanning Electron Microscope	56
3.5.4	Particle Size Analyser	57
3.5.5	Thermogravimetric Analysis	57
3.5.6	Differential Scanning Calorimetry	57
3.5.7	Total Porosity Estimation	58
3.5.8	Compression Test	58
3.5.9	Bioactivity Evaluation	59

CHAPTER FOUR : RESULTS AND DISCUSSION

4.1	Introduction	63
4.2	Characterisation of Starting Material	63
4.2.1	Polyurethane Foam	63
4.2.1(a)	SEM Observation	64
4.2.1(b)	Thermogravimetric Analysis	65
4.2.2	Beta Tricalcium Phosphate Powder	66
4.2.2(a)	Chemical Phase Analysis	66
4.2.2(b)	Particle Size Analysis and FESEM Observation	69
4.3	Fabrication of β -TCP Scaffold via PU Sponge Replica Method	71
4.3.1	Effect of Sintering Temperature	72
4.3.1(a)	Morphology Observation	72
4.3.1(b)	XRD Analysis	76
4.3.1(c)	FTIR Analysis	78

4.3.1(d) Total Porosity	80
4.3.2 Effect of β -TCP to Water Ratio	81
4.3.2(a) Morphology observation	82
4.3.2(b) Total Porosity	88
4.3.3 Effect of Binder Addition to β -TCP Slurry	89
4.3.3(a) Morphology Observation	89
4.3.3(b) Total Porosity	95
4.4 Biopolymer Coating	97
4.4.1 Characterisation of the Biopolymer	98
4.4.2 Morphology Observation	99
4.4.2(a) Excess Polymer Solution Removal	100
4.4.2(b) Morphology of β -TCP/PVA, β -TCP/PLA and β - TCP/PVA/PLA	101
4.4.2(c) Discussion	108
4.4.3 Coating Weight Percentage and Compressive Strength	110
4.5 Bioactivity Evaluation	115
CHAPTER FIVE : CONCLUSIONS	
5.1 Conclusion	127
5.2 Recommendation of Future Research	128
REFERENCES	129
LIST OF PUBLICATIONS	

LIST OF TABLES

		Page
Table 2.1	List of calcium phosphate bioceramic (Vallet-Regi, 2014; Dorozhkin, 2010a; Berzina-Cimdina & Borodajenko, 2012).	19
Table 2.2	List of calcium phosphate bioceramic (Vallet-Regi, 2014; Dorozhkin, 2010a; Berzina-Cimdina & Borodajenko, 2012).	21
Table 2.3	Comparison of natural and synthetic biopolymer (Mallick, 2014; Dorozhkin, 2011a; Kim et al., 2000; Tamariz & Rios-ramírez, 2013; Rezwan et al., 2006; Vroman & Tighzert, 2009; Gomes & Reis, 2004)	24
Table 2.4	Degradation of biopolymer implant (Lyu & Untereker, 2009; Marin et al., 2013).	25
Table 2.5	Properties of some biodegradable polymer and their degradation time (Dorozhkin, 2011a).	26
Table 2.6	Properties and characteristic of PLA (Armentano et al., 2010; Pawar et al., 2014).	36
Table 3.1	Order, amounts, formula weights of reagents for preparing 1000 ml of SBF.	40
Table 3.2	Composition of binder PVA and PEG added into β -TCP slurry.	45
Table 3.3	Sample codes of β -TCP biocomposites with different coating composition.	48
Table 3.4	Differences of ionic concentration and pH between human blood plasma and SBF (Kokubo & Takadama, 2006).	60
Table 4.1	Bands and the representative of present bonding in Figure 4.10 (Berzina-Cimdina & Borodajenko, 2012; Carrodegua & De Aza, 2011).	78

Table 4.2 Main PO₄ bands and their characteristic wavenumber in α-TCP and β-TCP in FTIR (Carrodeguas & De Aza, 2011) 80

LIST OF FIGURES

	Page
Figure 1.1	Flowchart of the overall research work. 6
Figure 2.1	Structure of mineralised collagen fibril (Cui et al., 2007). 8
Figure 2.2	Hierarchical structure of bone (Wegst et al., 2015). 10
Figure 2.3	Bone cellular structure: osteoblast, osteoclast and osteocyte (Imai et al., 2013). 12
Figure 2.4	Radiograph of (a) open tibial fracture with segmental bone loss, (b) after internal fixation and filled with cement spacer at the damaged tibia, (c) the defect after 3 and (d) 4 months. Bone healing never occurred (Pilia et al., 2013). 14
Figure 2.5	Regeneration of new bone tissue by the facilitation of bone scaffold substitute at the bone lost side (Mohamed & Shamaz, 2015). 15
Figure 2.6	Scanning Electron Microscope (SEM) image of HA/TCP bioceramic surface shows apatite layer formation before (left) and after (right) one day of immersion in SBF (Xin et al., 2005). 18
Figure 2.7	Cancellous bone (left), which has fully interconnected porous structure and internal open porous structure of PU sponge (right) (Ishikawa, 2010; Miao et al., 2008). 31
Figure 2.8	Procedures of the fabrication of α -TCP foam (Ishikawa, 2010) 32
Figure 2.9	SEM observation on ceramic strut after sintering (Kim et al., 2011). 34
Figure 2.10	Conversion of lactic acid to poly(lactic acid) (McKeen, 2014). 35
Figure 2.11	Partial (left) and fully (right) hydrolysed of PVA (DeMerlis & Schoneker, 2003). 37

Figure 3.1	Flow chart of β -TCP scaffold fabrication.	42
Figure 3.2	Sintering profile of β -TCP coated polyurethane sponge.	43
Figure 3.3	Overall flowchart of PVA and/or PLA coating on β -TCP scaffold.	47
Figure 3.4	Flowchart of PVA solution coating on β -TCP scaffold.	50
Figure 3.5	Set up of Büchner funnel and flask to remove excess polymer solution via vacuum suction at reduced pressure.	51
Figure 3.6	Flowchart of PLA solution coating on β -TCP scaffold.	52
Figure 3.7	Flowchart of PVA and PLA bi-layer coating on β -TCP scaffold.	53
Figure 3.8	Schematic diagram of compressive strength test.	59
Figure 3.9	Illustration of β -TCP samples soaked in SBF solution.	62
Figure 4.1	SEM observation of polyurethane foam.	64
Figure 4.2	TGA of PU sponge (solid line represented the mass percentage with heating temperature; dotted line represent the derivatives of the solid line, DTG).	65
Figure 4.3	XRD pattern of the starting β -TCP powder.	67
Figure 4.4	FTIR spectrum of starting β -TCP powder.	68
Figure 4.5	Particle size distribution of β -TCP powder.	69
Figure 4.6	Starting powder of β -TCP under FESEM observation (arrows show the fusion of particles).	70
Figure 4.7	SEM microscopic images of β -TCP scaffold sintered at 1100°C (a, b), 1200°C (c, d), 1250°C (e, f) and 1300°C (g, h).	73
Figure 4.8	Range of pore size of β -TCP scaffold after sintering.	75
Figure 4.9	XRD spectra of β -TCP before sintering and sintered at 1100, 1200, 1250 and 1300°C.	77

Figure 4.10	FTIR spectra of β -TCP before sintering and sintered at 1100°C, 1200°C, 1250°C and 1300°C.	78
Figure 4.11	Total porosity of β -TCP foam sintered at 1100°C, 1200°C, 1250°C and 1300°C.	80
Figure 4.12	Macrostructure of β -TCP scaffold sintered at 1100°C, 1200°C, 1250°C and 1300°C produced by 10g:10ml and 10g:8ml of slurries (arrow marks the cracks).	83
Figure 4.13	Estimated strut thickness of the β -TCP scaffold prepared from ratio 10g:10ml and 10g:8ml of slurry and sintered at 1100°C, 1200°C, 1250°C and 1300°C.	84
Figure 4.14	Macrostructure of β -TCP scaffold sintered at 1250°C produced by 10g:6ml slurry (arrows pointed the clogged macropores).	85
Figure 4.15	Microstructure of β -TCP scaffold sintered at 1100°C, 1200°C, 1250°C and 1300°C produced by 10g:10ml and 10g:8ml of slurries.	87
Figure 4.16	Total porosity of β -TCP scaffold sintered at 1100°C, 1200°C, 1250°C and 1300°C produced by 10g:10ml and 10g:8ml of slurries.	88
Figure 4.17	SEM observation of β -TCP scaffolds with different composition of binder.	91
Figure 4.18	Comparison of macro- and microstructure of β -TCP scaffold produced with binder PVA and PEG addition in the slurry (crack pointed by arrow).	93
Figure 4.19	Estimated strut thickness of the β -TCP scaffold produced with binder PVA and PEG addition in the slurry.	95
Figure 4.20	Comparison of total porosity of β -TCP scaffold with the loading of PVA and PEG binder.	96
Figure 4.21	DSC analysis of PLA and PVA.	99

Figure 4.22	Comparison of PVA coating on β -TCP scaffold after sprayed with air gun (a and b) and vacuum suction at reduced pressure (c and d) to remove excess polymer solution.	100
Figure 4.23	SEM observation of sample V1, (a) near to surface, magnification 60 X; (b) near to surface, magnification 1k X; (c) interior, 60 X and (d) interior, 1k X.	102
Figure 4.24	SEM observation of sample V3, (a) near to surface, magnification 60 X; (b) near to surface, magnification 1k X; (c) interior, 60 X and (d) interior, 1k X.	103
Figure 4.25	SEM observation of sample V5, (a) near to surface, magnification 60 X; (b) near to surface, magnification 1k X; (c) interior, 60 X and (d) interior, 1k X.	103
Figure 4.26	SEM observation of sample V10, (a) near to surface, magnification 60 X; (b) near to surface, magnification 1k X; (c) interior, 60 X and (d) interior, 1k X.	104
Figure 4.27	SEM observation of sample L5, (a) near to surface, magnification 60 X; (b) near to surface, magnification 1k X; (c) interior, 60 X and (d) interior, 1k X.	104
Figure 4.28	SEM observation of sample V1_L5, (a) near to surface, magnification 60 X; (b) near to surface, magnification 1k X; (c) interior, 60 X and (d) interior, 1 k X.	106
Figure 4.29	SEM observation of sample V3_L5, (a) near to surface, magnification 60 X; (b) near to surface, magnification 1k X; (c) interior, 60 X and (d) interior, 1k X.	106
Figure 4.30	Cross sectional SEM image of β -TCP and β -TCP/polymer strut (a) without polymer coating, (b) V5, (c) L5 (d) V1_L5 and (e) V3_L5.	108
Figure 4.31	Coating weight percentage of β -TCP-biopolymer scaffolds after coating with different composition of PVA and/or PLA.	110

Figure 4.32	Compressive strength of β -TCP scaffolds after coating with different composition of PVA and/or PLA.	111
Figure 4.33	SEM observation of fracture strut before and after PVA and/or PLA coating; (a) non coated β -TCP, (b) V1, (c) V3, (d) V5, (e) V10, (f) L5, (g) V1_L5 and (h) V3_L5.	113
Figure 4.34	FESEM images of pure β -TCP scaffold immersed in SBF for 3 days (a & b), 1 week (c & d), 2 weeks (e & f), 4 weeks (g & h) and 6 weeks (i & j), apatite pointed by arrows.	116
Figure 4.35	“Cauliflower” or flaky-like morphology of apatite nuclei.	118
Figure 4.36	FESEM images of V5 immersed in SBF for 1 week (a & b), 2 week (c & d), 4 weeks (e & f), and 6 weeks (g & h).	119
Figure 4.37	FESEM images of L5 immersed in SBF for 1 week (a & b), 2 week (c & d), 4 weeks (e & f), and 6 weeks (g & h).	120
Figure 4.38	FESEM images of V3_L5 immersed in SBF for 1 week (a & b), 2 week (c & d), 4 weeks (e & f), and 6 weeks (g & h).	122
Figure 4.39	Weight gain and loss trend of β -TCP, V5, L5 and V3_L5 immersion in SBF from 1 to 6 weeks.	124
Figure 4.40	pH variation of β -TCP, V5, L5 and V3_L5 immersion in SBF from 1 to 6 weeks.	125

LIST OF SYMBOLS

α	Alpha
β	Beta
$^{\circ}$	Degree
D_f	Final diameter
t_f	Final thickness
D_i	Initial diameter
t_i	Initial thickness
θ	Theta
wt. %	Weight Percentage
μm	Micrometre

LIST OF ABBREVIATIONS

α -TCP	Alpha Tricalcium Phosphate
β -TCP	Beta Tricalcium Phosphate
β -CPP	Beta Calcium Pyrophosphate
BCP	Biphasic Calcium Phosphate
CaP	Calcium Phosphate
Ca/P	Calcium-to-Phosphate ratio
DSC	Differential Scanning Calorimeter
FESEM	Field Emission Scanning Electron Microscope
FTIR	Fourier Transform Infra-Red
HA	Hydroxyapatite
ICDD	International Centre for Diffraction Data
M_w	Weight Average Molecular Weight
PLA	Poly (Lactic Acid)
PVA	Poly (Vinyl Alcohol)
PSA	Particle Size Analyser
PU	Polyurethane
SBF	Simulated Body Fluid
TCP	Tricalcium Phosphate
TGA	Thermogravimetric Analysis
TE	Tissue Engineering
XRD	X-ray Diffraction

FABRIKASI KERANGKA TULANG 3D BERLIANG BETA TRIKALSIMUM FOSFAT BERSALUT POLI(VINIL ALKOHOL) DAN POLI(LAKTIK ASID)

ABSTRAK

Kerangka β -TCP yang bersambungan liang telah dihasilkan dengan cara replika busa poliuretana. Kerangka tersebut kemudian disalut dengan PVA dan PLA untuk meningkatkan kekuatan mampatannya. Kajian di peringkat pertama adalah pengoptimuman rangkaian dalaman kerangka β -TCP (dengan pengurangan kecacatan) sebelum disalut dengan polimer bio. Kerangka yang terhasil daripada buburan β -TCP dan air dalam nisbah 10g:8ml dengan penambahan 2 wt. % PVA dan PEG, dan disinter pada 1250°C selama 2 jam mempunyai makro- dan mikroliang yang optimum. Kerangka optimum yang terhasil mempunyai keporosan sebanyak 95.3%, tanpa makroliang tersumbat dan mempunyai topang yang berketebalan sekata serta rekahan yang minimum. Dalam proses penyalutan polimer bio di kajian peringkat kedua, penyalutan dengan PVA berkepekatan tinggi menyebabkan makroliang tersumbat manakala penyalutan dengan PVA berkepekatan rendah menyebabkan topang di bahagian tengah sampel gagal disalut. PLA kemudian digunakan sebagai lapisan dwi-salutan kepada sampel yang disalut oleh PVA berkepekatan rendah. Dari aspek mekanikal, kekuatan mampatan kerangka meningkat apabila berat peratusan polimer yang disalut bertambah. Peregangan polimer di antara retakan menunjukkan mekanisme titian retakan yang memperkuatkan kerangka β -TCP yang rapuh. Kerangka yang disalut dengan 3 wt. % PVA dan seterusnya dengan 5 wt. % PLA (V3_L5) mempunyai kekuatan mampatan tertinggi (83.7 kPa) tanpa sumbatan makroliang. Dari segi bioaktiviti, β -TCP mengambil masa 2 minggu untuk pembentukan apatit dalam SBF tetapi V3_L5 mengambil masa selama 4 minggu. Ini menunjukkan PLA yang hidrofobik melanjutkan masa pembentukan apatit.

**FABRICATION OF 3D POROUS β -TRICALCIUM PHOSPHATE BONE
SCAFFOLD COATED BY POLY(VINYL ALCOHOL) AND
POLY(LACTIC ACID)**

ABSTRACT

The interconnected porous β -TCP scaffold was produced via polyurethane (PU) foam replica method. PVA and/or PLA were coated on the scaffold to enhance the compressive strength. The first part of this study was to optimise the internal architecture of β -TCP scaffold with minimal defect before biopolymer coating. Optimum macro- and microporosity in β -TCP scaffold were produced by slurry with ratio 10g:8ml of powder to water and addition of 2 wt. % of PVA and PEG and sintered at 1250°C for 2 hours. The optimum scaffold had 95.3% of porosity with unblock macropore, minimum crack and regular thickness of strut. In the second part, during biopolymer coating, single layer coating with higher PVA concentration had macropores blockage, while lower PVA concentration coating showed uncoated at interior of the scaffold. Bi-layer coating with PLA was to compensate the uncoated interior region in lower PVA concentration coated sample. In terms of mechanical property, compressive strength of the coated scaffold increased with the coated weight percentage of biopolymer. Polymer stretched at the crack opening showed crack bridging mechanism, which toughened the brittle β -TCP scaffold. Scaffold bi-layer coated with 3 wt. % of PVA and subsequently 5 wt. % PLA (V3_L5) had the highest compressive strength (83.7 kPa) with no macropore blocking by biopolymer. In terms of bioactivity, β -TCP without biopolymer coating took 2 weeks to form apatite but V3_L5 took 4 weeks after immersion in SBF. This showed that coating with hydrophobic PLA delayed the time of apatite formation.

CHAPTER ONE

INTRODUCTION

1.1 Research Background

Human body is susceptible to damage or deterioration due to aging, accidents or disease factors. Some losses such as the loss of limbs and teeth, organs like kidney or brain are permanent as our body is unable to regenerate it. So, necessity of lose organ replacement triggers the continuous advancement in biomedical area, such as tissue engineering. The main subject in this study is the replacement materials for the bone. Bone is one important organ in our body, which it plays important roles in critical functions in human physiology including protection, movement, support of other critical organs, blood production, blood pH regulation, mineral storage and homeostasis (Mohamed & Shamaz, 2015).

Orthopaedic fracture of bone is very common and our bone is very unique with its self-healing ability, with modern medical treatment it can heal without much problem. However, when large bone portion was removed due to diseases or trauma, bone regeneration would be disturbed and it is far beyond the ability of self-healing leading to complication associated with delayed union or fracture non-union (Gómez-Barrena et al., 2015; Pilia et al., 2013; Jones & Hench, 2003). As a treatment to these bone defects, the alternative is to replace the bone loss portion with bone scaffold.

Traditional tissue implantation (i.e. autographs, allographs, and xenographs) has been the source of bone grafting replacement. However, their limitations are donor site undersupply, high rejection rate, disease transfer, harvesting cost and postoperative morbidity. So, current approach is to replace biological material with synthetic

materials (Oryan et al., 2014; Keating & Mcqueen, 2001; Navarro et al., 2008). A synthetic bone scaffold has to be biocompatible, bioresorbable, porous with interconnected pores, having sufficient mechanical stability and bioactive in order to trigger cell response as well as assist in bone healing (Pilia et al., 2013). Engineering team combines the material selection and fabrication technology in scaffold construction to fulfil the requirements (Mohamed & Shamaz, 2015).

Similarly, fabrication of a ceramic-polymer bone scaffold was embark to mimic the structure of natural human bone, which consists of interpenetrating of inorganic hydroxyapatite and biological collagen (Mohamed & Shamaz, 2015). However, challenges exist as to combine ceramic and polymer since processing temperature for these two materials are distinctly different. Hence polymer coated ceramic framework method has been suggested to overcome this shortcoming. Besides, polymer is a ductile material, the addition of polymer phase hence was intended to reduce the brittleness of β -TCP ceramic phase. Similar works showing the improvement of mechanical strength have been reported by Bang et al. (2013) of poly (ϵ -carpolactone) (PCL) coated α -TCP, Miao et al. (2007) of PLGA coated HA/TCP and Nie et al. (2012) of BCP multiply coated by HA/PLLA.

Among fabrication techniques, polyurethane (PU) sponge replica method is the straightforward and simple method to produce a porous structure scaffold. Spongy architecture of the PU provides the replication template to produce an interconnected and macroporous ceramic scaffold (Mohamad-Yunos et al., 2008). Although trade-off between mechanical strength and porous structure existed, to combine with polymer phase, the polymer coating uses the distinct interconnected porous characteristic produced via this sponge replication method, to infiltrate into the ceramic framework to enhance the toughness of ceramic phase.

In terms of materials selection, hydroxyapatite (HA) resembles the chemical composition with inorganic phase of bone, and hence it is often the prime candidate of bone scaffold material (Dorozhkin, 2011b; Barakat et al., 2008). But HA has low bioresorption rate. A relatively resorbable beta-tricalcium phosphate (β -TCP) instead is a more promising material to construct a bone scaffold (Liu & Lun, 2012; Sohier et al., 2010). A resorbable implant is a better regeneration route to replace the substituted part with bone tissue in a slowly manner (Alves et al., 2010; Giannoudis et al., 2005). In addition, β -TCP with Ca/P ratio of 1.5 is within the range of human bone than pure HA (Ca/P ratio of human bone is 1.3 to 1.66, depending on the person's age) (Horowitz et al., 2010).

In the case of the polymer phase, poly(vinyl alcohol) (PVA) and poly(lactic acid) (PLA) are two examples of biocompatible and biodegradable polymers being developed in medicine and pharmaceutical application. PVA was reported to be elastic (Tamariz & Rios-ramírez, 2013; Asran et al., 2010) and its combination with ceramic scaffold significantly enhanced the scaffold mechanical strength (Song et al., 2011; Degirmenbasi et al., 2006). PLA was also reported having excellent mechanical property due to its crystallinity and hence being used in biomedical application (Davachi & Kaffashi, 2015; Pawar et al., 2014; Savioli-Lopes et al., 2012).

1.2 Problem Statement

Although HA resembles the mineral phase of human, β -TCP was used instead due to the relatively balanced resorption and bone regeneration rate (Liu & Lun, 2012). It is reported that a porous scaffold of total porosity 70-95% with interconnected pores of diameter ranging from 200-900 μ m is beneficial for bone growth and vascularisation (Asaad et al., 2016; Pilia et al., 2013). In this study, polyurethane (PU) sponge replica

method was employed to produce a β -TCP scaffold which has high porosity with 3 dimensional interconnected porous structure. However, the porosity affects the mechanical properties of the scaffold, where the compressive strength decreases as the porosity increases. Therefore incorporation with ductile polymer was hypothesised to be able to enhance the toughness of β -TCP scaffold (Asaad et al., 2016; Kang et al., 2011).

In the first part of this study involving the bioceramic framework fabrication, the PU sponge replica method involves coating of the PU sponge with the β -TCP slurry and this was followed by burning out of the PU template through sintering. The properties of the β -TCP scaffold (i.e. strut appearance) were related to the condition of slurry and sintering profile (Monmaturapoj & Yatonchai, 2011; Mohamad-Yunos et al., 2008). Hence, sintering and slurry condition were studied to optimise the internal architecture (macro-, microporosity, total porosity and morphology of the strut) of the β -TCP scaffold. The β -TCP framework optimising is important to reduce as many defect point (i.e. crack) as possible before the work proceed to biopolymer coating in the second part.

One approach to strengthen the mechanical strength of the porous scaffold is to coat with polymer layer (Asaad et al., 2016; Kang et al., 2011). In biopolymer coating, the biopolymer solution was not only coated on the strut surface but was made to fill the existing micropores in the bioceramic scaffold forming the interpenetrating network within the β -TCP framework (Mohamad-Yunos et al., 2008). The biopolymer phase also acts as a binder to hold the ceramic phase, which would bridge cracks during fracture subsequently increasing the scaffold toughness.

As reported that the combination of ceramic scaffolds with PLA (Martínez-Vázquez et al., 2014) and with PVA (Song et al., 2011) improved the mechanical strength

of the materials, hence in this study compressive strength of β -TCP scaffolds coated with these two biopolymers (single and bi-layer of PVA and PLA) were compared. Adding that synthetic biopolymer was reported as not bioactive (Asaad et al., 2016; Boccaccini et al., 2013), the bioactivity of hydrophilic PVA and/or the hydrophobic PLA coating on the bioactive bioceramic were being investigated via immersion in SBF for a period of time.

1.3 Research Objective

The aim of this study is to develop bioceramic-biopolymer scaffold made up of β -TCP, PVA and PLA, which leads to the following objectives:

- i. To fabricate β -TCP scaffold by polyurethane sponge replica method.
- ii. To optimise the internal architecture of β -TCP scaffold through the effect of sintering condition, ratio of β -TCP to water and addition of binder.
- iii. To improve the compressive strength of β -TCP scaffold by biopolymer coating.
- iv. To evaluate the *in vitro* bioactivity of β -TCP scaffold before and after biopolymer coating.

1.4 Scope of Research

This study was divided into three stages: started from the optimising fabrication study of β -TCP scaffold, followed by the PVA and/or PLA coating, and lastly bioactivity evaluation of the scaffold before and after polymer coating. Internal architecture of β -TCP scaffold produced in first stage is important to have minimum undesired defect before proceeded to next stage. Also, fabrication process determines the microporosity structure of the β -TCP matrix, which enable the interpenetration of polymer and β -TCP phase. Flow chart of this study is shown in Figure 1.1.

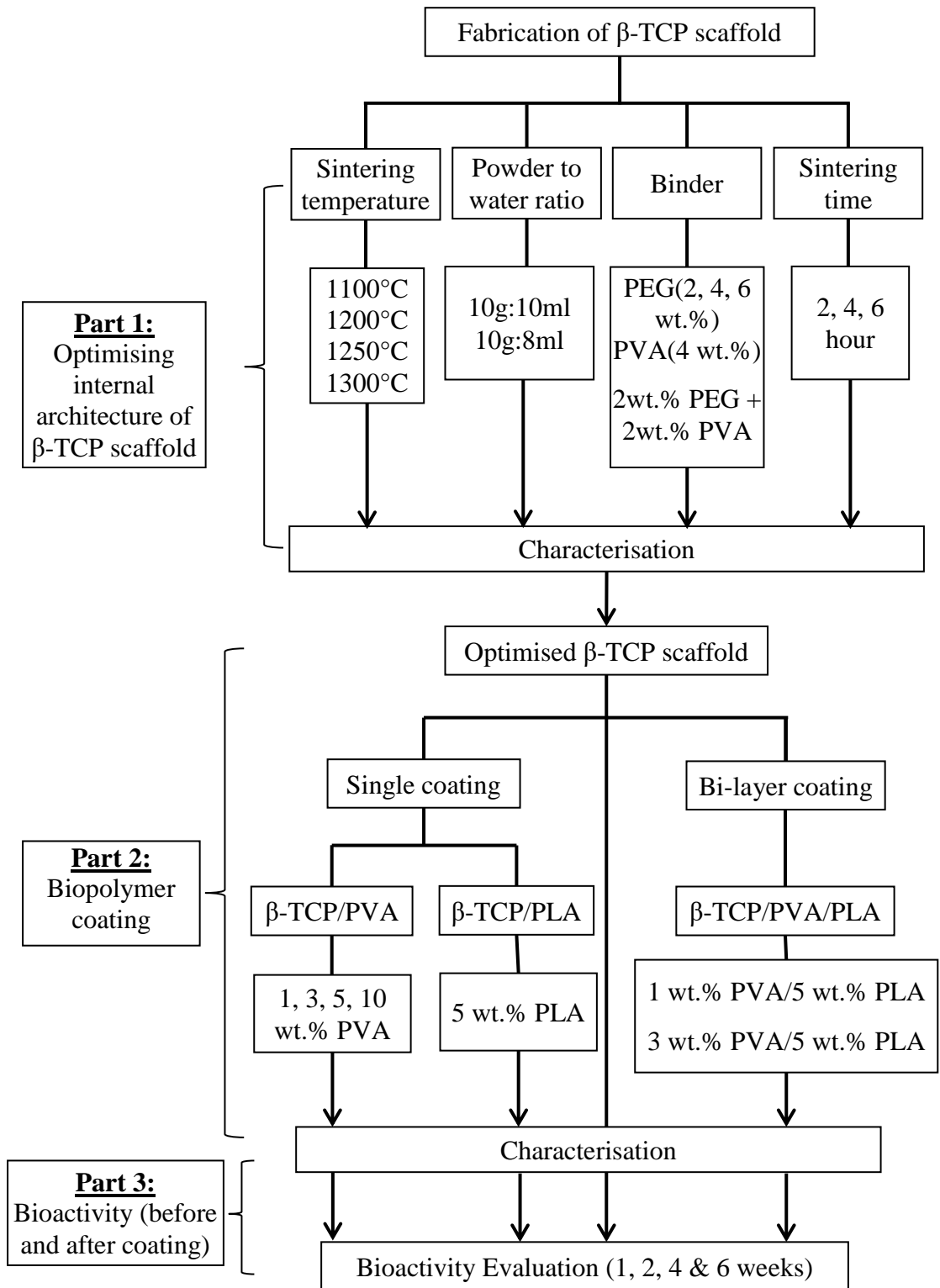


Figure 1.1 Flowchart of the overall research work.

CHAPTER TWO

LITERATURE REVIEW

2.1 Introduction

This research work focuses on fabrication of synthetic bone scaffold as the alternative to tissue transplantation for orthopaedic injury treatment. In order to produce a scaffold biomimetic to bone, this chapter starts with a brief insight of hard tissue mineralisation, bone structure and remodeling process. It is then followed by bone scaffold for orthopaedic. After understanding the requirements of an ideal bone scaffold, materials selection and fabrication techniques of synthetic bone scaffold, particularly bioceramic and biopolymer and their combination are discussed. Lastly, β -TCP scaffold coated with PVA and PLA are presented and discussed.

2.2 Hard Tissue Mineralisation

Bone, dentin and dental enamel are the hard tissues existed in human body (Brien, 2011). Dentin and enamel are the substances that constitute the inner and outer layer of the teeth while bone is a hard endoskeletal connective tissue composed of inorganic mineral HA. The similarity between these hard tissues is they are made from natural calcium phosphate ceramics (Dorozhkin, 2011b).

Basic unit of bone tissue is a mineralised collagen fibril (refer to Figure 2.1). Bone tissues are produced by a series of natural biomineralisation process, which is also known as calcification, indicating that accumulation or precipitation of calcium to form bone (Alves et al., 2010). Collagen fibrils are formed by self-assembly of collagen triple helices, it acts as the template for the nucleation of HA nanocrystals on